Ceramics International 47 (2021) 15039–15043

Contents lists available at ScienceDirect

Ceramics International

journal homepage: www.elsevier.com/locate/ceramint

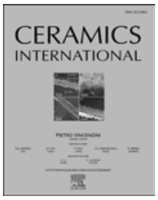

Enhancement of structural and microwave properties of Zn^{2+} ion-substituted Li_2MgSiO_4 ceramics for LTCC applications

Jie Li [a,*], Haokai Su [a], Yahui Sun [a], Gang Wang [a], Feng Gao [a], Xuening Han [a], Zheng Liang [a], Qiang Li [b]

[a] *State Key Laboratory of Electronic Thin Film and Integrated Devices, University of Electronic Science and Technology of China, Chengdu, 610054, China*
[b] *School of Instrument and Electronics, North University of China, Taiyuan, 030000, China*

ARTICLE INFO

Keywords:
Li_2MgSiO_4 ceramics
Zn^{2+} substitution
Microwave dielectric properties
LTCC applications

ABSTRACT

In this study, Zn^{2+}-substituted Li_2MgSiO_4 ceramics ($Li_2(Mg_{1-x}Zn_x)SiO_4$, x = 0.00, 0.05, 0.10, 0.15, and 0.20) were synthesized using a traditional solid-state method. A fixed amount of LiF sintering aid (1.5 wt%) was added to the ceramics for decreasing the sintering temperature and adjusting their microwave dielectric properties. X-ray diffraction (XRD) results revealed no secondary phases, and scanning electron microscopy (SEM) data suggest that the Zn^{2+} ion substitution increased the size and uniformity of the grains, thereby affecting the densification of the prepared ceramics. The maximum bulk density (2.94 g/cm^3) was found in a Zn^{2+} ion-substituted ceramic with x = 0.10 at a relative density of 94.2% (compared with the XRD theoretical density). Excellent microwave dielectric properties ($\varepsilon_r = 6.28$, $Q \times f = 50400$ GHz, and $\tau_f = -145$ ppm/°C) can also be obtained at this zirconium content. We believe that the developed ceramics are promising for use as antenna substrates or transmit/receive modules in low-temperature co-firing ceramic applications.

1. Introduction

With a long-standing foundation in wireless communication, the technological innovation of antennas has evolved with the world of technology. As an essential aspect of fifth generation (5G) networks, antenna design is one of the most rapidly growing state-of-the-art industries [1]. In particular, smartphone and cellular phone antenna design- and their transformation from external to built-in antennas has become a large and high-performing market [2–4]. Low temperature co-fired ceramics (LTCC) technology is an effective way to produce multilayer electron devices in communication systems. The internal electrodes in these communication systems are comprised mainly of silver owing to its excellent conductivity. However, the high melting point of silver (961 °C) limits the maximum firing temperature of ceramics [5–7]. Therefore, researches into sintering aids have increased, as they allow for lower sintering temperatures. In recent years, there has been increasing interest in low-temperature co-fired ceramics (LTCC) with silicate structure. Their reduced dielectric loss and dielectric constant and high quality factor make these materials the most preferred substrates for microwave communication applications [8–11]. To date, research have focused largely on forsterite (Mg_2SiO_4) [12], lithium magnesium silicate (Li_2MgSiO_4) [13], wollastonite ($CaSiO_3$), and zinc silicate (Zn_2SiO_4) [14] among others [15–17]. Following from these studies, this study aims to further explore the effects of Zn^{2+} ion substitution on the structural and microwave dielectric properties of $Li_2(Mg_{1-x}Zn_x)SiO_4$ ceramics.

2. Experimental

Li_2CO_3, MgO, ZnO, and SiO_2 AR purity oxides were used as raw materials. $Li_2(Mg_{1-x}Zn_x)SiO_4$ ceramics (x = 0.00, 0.05, 0.10, 0.15, and 0.20) were prepared via a conventional solid-state reaction. For this, the oxide powders were exposed to 18 h of milling in distilled water with ZrO_2 balls. They were then dried and calcined for 2 h in air at 1000 °C. These powders were re-milled for 12 h with 1.5 wt% LiF sintering aid and dried at 100 °C. After that, the powders were mixed with 20 wt% PVA as a binder, pressed into disks under a pressure of 10 MPa, and sintered at 900 °C for 4 h.

The crystalline phase of the samples was identified by X-ray diffraction (XRD) with a DX-2700 diffractometer (Haoyuan Co.) using Cu–Kα radiation. The microstructure of sintered ceramics was investigated through scanning electron microscopy (SEM) using a Zeiss INCA

---

[*] Corresponding author.
E-mail address: lijie@uestc.edu.cn (J. Li).

https://doi.org/10.1016/j.ceramint.2021.02.060
Received 25 November 2020; Received in revised form 29 January 2021; Accepted 5 February 2021

Penta FETX 3 microscope (Oxford Instruments). The bulk density of ceramics was measured using a GF-300D auto-density tester (A&D Co.) based on the Archimedes method. The microwave dielectric properties of the sintered samples were evaluated using an Agilent N5230A (300 MHz–20 GHz) network analyzer in the resonant cavity mode. The temperature coefficient of the resonant frequency (τ_f) was measured via the open cavity method in a temperature range of 20–80 °C. The τ_f parameter was calculated using the formula below:

$$\tau_f = (f_{80} - f_{20})/\{ f_{20} \times f_{80}\} \times 10^6 \text{ (ppm/°C)},$$

where f_{80} and f_{20} are the resonant frequencies at 80 and 20 °C, respectively. All the experiments were performed at room temperature (25 °C).

3. Results and discussion

Fig. 1 describes the XRD patterns of the samples as a function of the Zn^{2+} ion content. All the studied compounds exhibit emergence of diffraction peaks whose phases directly correspond to those of undoped Li_2MgSiO_4 (ICDD-PDF, 24–0636), implying that no secondary phases were formed during sintering and that the Zn^{2+} ion substitution had no significant effect on the phase structure of the ceramics. However, an increase in the Zn^{2+} ion concentration noticeably increases the peak intensity, confirming the transformation of lattice parameter due to the difference in the ionic radii of Zn^{2+} and Mg^{2+}. This means that the crystalline phase of the ceramics remained unchanged and Zn^{2+} ions were successfully settled at the lattice sites of Mg^{2+} ions.

Fig. 2 shows the SEM micrographs of $Li_2(Mg_{1\text{-}x}Zn_x)SiO_4$ samples with different Zn^{2+} ion contents. Pure Li_2MgSiO_4 ceramic ($x = 0$) has a small grain size (approximately 2–3 μm), with pores between the grain boundaries. The use of LiF sintering aid lowers the sintering temperature (900 °C) and promotes the phase formation but prevents the grain growth. Adding Zn^{2+} dopant in the ceramics causes an increase in the grain size (5–8 μm) and, consequently, a reduction in the degree of porosity. For dielectric materials, the dielectric constant could be defined using the formula below:

$$\varepsilon = \varepsilon_r + \varepsilon_{dw}$$

where ε_r is intrinsic dielectric constant, and ε_{dw} is domain wall dielectric constant. The contribution of ε_r was mainly from materials composition and grain size, and the contribution of ε_{dw} was mainly from domain wall gap. Hence, the grain size was bigger, the dielectric property was better. Meanwhile, the porosity was lower, the dielectric property was better. When $x = 0.00$–0.10, the grain size was uniform and it played a positive role in the dielectric property. When $x = 0.15$ and 0.20, the grain size became bigger and the porosity went up, and the bulk density decreased, which led to a negative effect on the dielectric property of ceramics.

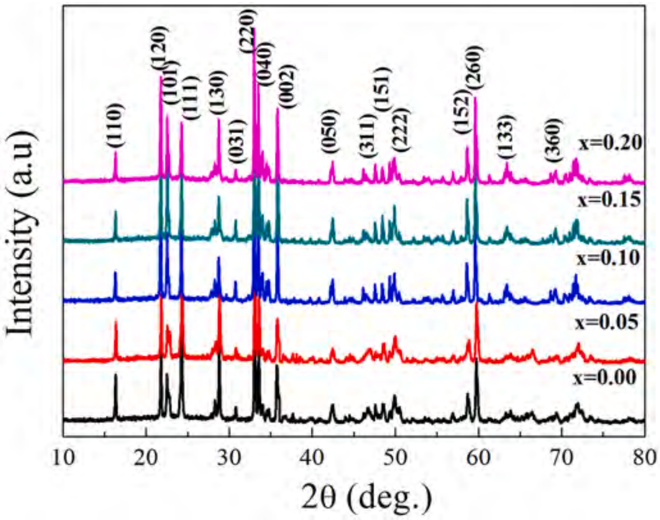

Fig. 1. XRD patterns of $Li_2(Mg_{1\text{-}x}Zn_x)SiO_4$ ceramics at various Zn^{2+} ion concentrations.

It is well established that the dielectric properties of ceramics are affected by their chemical composition and bulk density, the effects of which were found herein. Fig. 3 displays the theoretical density and bulk density of $Li_2(Mg_{1\text{-}x}Zn_x)SiO_4$ ceramics as a function of the Zn^{2+} dopant content. For all the samples, embedding Zn^{2+} ions results in a steady increase (at $x \leq 0.10$) and then a gradual decrease (at $x > 0.10$) in both parameters. The observed plots can be divided into two parts according to the phase composition provided by the XRD data. The first is associated with the high molecular weight of Zn^{2+} cations substituting Mg^{2+} ions. Based on the XRD data, the full theoretical densities of Li_2MgSiO_4 and Li_2ZnSiO_4 are 3.074 and 3.628 g/cm^3, respectively. Introducing Zn^{2+} ions increases the density of the Li_2MgSiO_4 composite. The maximum theoretical and bulk densities observed for a ceramic with $x = 0.10$ are 3.12 and 2.94 g/cm^3, respectively. A further increase in the Zn^{2+} cation content to $x = 0.15$ and 0.20 resulted in a decrease in both the parameters. The relative bulk density was found to be 94.2% when $x = 0.10$, which is in agreement with the SEM results shown in Fig. 2.

Fig. 4 shows the evolution of dielectric constant (ε) in samples with varying Zn^{2+} ion content. The relationship between the dielectric constant and the value of x exhibited the same trend as the density. The dielectric constant linearly increases in the range of $0 < x < 0.1$, and then decreases at $x > 0.10$. In ceramics, the dielectric constant ε is known to be dependent on the ionic polarizability of the composition, relative bulk density, and secondary phase [18]. In the case of pure $Li_2(Mg_{1\text{-}x}Zn_x)SiO_4$ ceramics, the dielectric constant was found to cover a low value range ($\varepsilon = 5$–8), determined by its chemical composition [19]. Furthermore, ε behaves similar to the relative density, i.e., it increases when zirconium dopants are added until $x = 0.10$, and then decreases with a further increase in the Zn^{2+} ion content. At $x < 0.10$, the introduction of zirconium cations into the ceramic causes a decrease in the degree of porosity, increasing the bulk density, as seen in Fig. 3, thus resulting in an increase in the dielectric constant. At $x > 0.10$, the bulk density decreases (Fig. 3), reducing ε. Moreover, doping induces lattice distortion, further decreasing the dielectric constant [20].

Fig. 5 shows the variation in the $Q \times f$ values of $Li_2(Mg_{1\text{-}x}Zn_x)SiO_4$ ceramics. It is obvious that the $Q \times f$ parameter exhibits an inverse trend to that of the dielectric constant for different concentrations of Zn^{2+} ions. The addition of Zn^{2+} ions caused the $Q \times f$ value to decrease from 59064 to 50300 GHz, due to alteration of the original crystalline structure of Li_2MgSiO_4 ceramics. A further increase in the zirconium cation content, to $x = 0.20$, led the quality parameter to increase to 61000 GHz. Because the microwave properties of LTCCs are determined by the grain size, bulk density, and secondary phases (if any), the $Q \times f$ parameter also is affected by the densification and grain uniformity of ceramics. At $x \leq 0.1$, the decrease in the $Q \times f$ value was due to small grain size and increasing bulk density (Fig. 3). In turn, at $x \geq 0.1$, the presence of Zn^{2+} ions promoted grain growth and increased the dielectric characteristics, enhancing the quality factor of the ceramics.

Fig. 6 demonstrates how the temperature coefficient (τ_f) of $Li_2(Mg_{1\text{-}x}Zn_x)SiO_4$ ceramics varies as a function of the Zn^{2+} ion content, within a temperature range of 20–80 °C. As seen in Fig. 6, τ_f gradually increases with zirconium cation concentration. Temperature stability is very important when producing microwave dielectric ceramics. Typically, the higher the temperature, the lower the Q value of the material. For a dielectric material, the temperature coefficient of the dielectric constant (τ_ε) is generally defined as

$$\tau_\varepsilon = \frac{1}{\varepsilon_r}\frac{d\varepsilon_r}{dT}.$$

While constructing dielectric ceramics, τ_f of the material should be compensated for by choosing a suitable thermal expansion coefficient (α). This will ensure the stability of the device at high temperatures, with an applied frequency. Hence, the temperature coefficient of the resonant

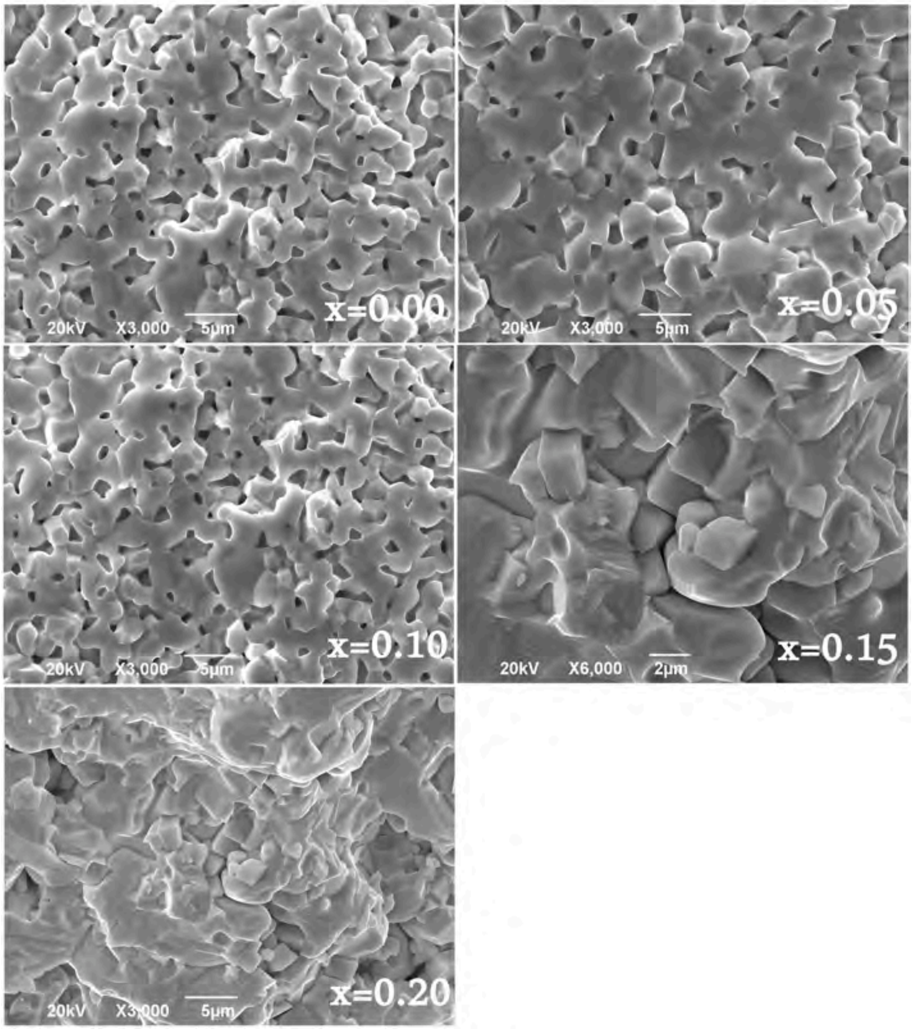

Fig. 2. SEM images of $Li_2(Mg_{1-x}Zn_x)SiO_4$ ceramics at different Zn^{2+} ion concentrations *x*.

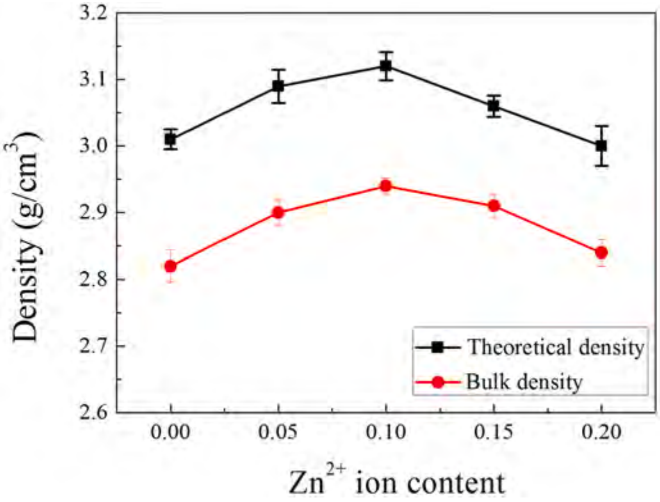

Fig. 3. Theoretical density and bulk density of $Li_2(Mg_{1-x}Zn_x)SiO_4$ ceramics vs. Zn^{2+} ion concentration *x*.

frequency (τ_f) is related to τ_ε by the following relationship:

$$\tau_f = -\alpha - \frac{1}{2}\tau_\varepsilon.$$

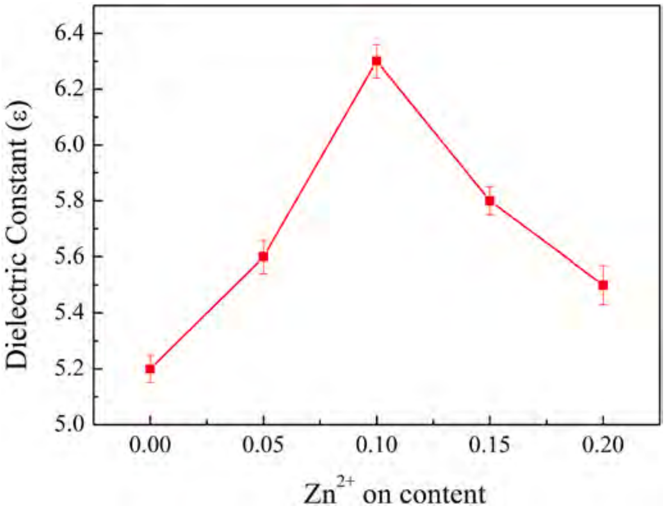

Fig. 4. Dielectric constant of $Li_2(Mg_{1-x}Zn_x)SiO_4$ ceramics with varying Zn^{2+} ion contents.

Generally, the temperature coefficient of ceramic materials should be nearly zero. However, the thermal expansion coefficient (α) of ceramics is positive, with a value of ~6–10 ppm/°C. Changing the

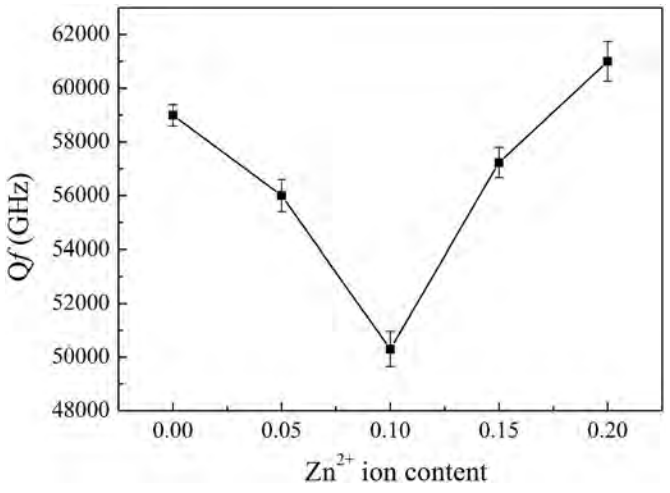

Fig. 5. $Q \times f$ parameter of $Li_2(Mg_{1-x}Zn_x)SiO_4$ ceramics at different Zn^{2+} ion contents.

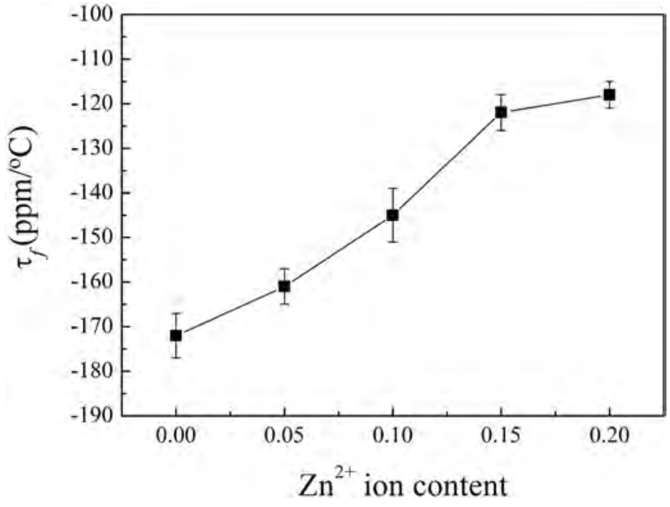

Fig. 6. τ_f parameter vs. Zn^{2+} ion content in $Li_2(Mg_{1-x}Zn_x)SiO_4$ ceramics.

sintering temperature did not alter the crystal structure, proving that the value of α can be regarded as constant. Therefore, the relationship between τ_f and ε_r can be expressed by the following equation:

$$\tau_f = -\alpha - \frac{1}{2\varepsilon_r}\frac{d\varepsilon_r}{dT} \propto \varepsilon_r.$$

This equation demonstrates the close relationship between τ_ε and ε_r. As shown in Fig. 6, the value of τ_f increased with Zn^{2+} ion levels. Compared to the Li_2MgSiO_4 ceramic (−170 ppm/°C), the Li_2ZnSiO_4 ceramic had a less negative τ_f value (−47.2 ppm/°C) [21], which could be the reason for the results of the present experiment. Therefore, an appropriate τ_f value could be obtained with higher Zn^{2+} ion levels. When x = 0.2, $\tau_f = -120$ ppm/°C. Hence, through Zn^{2+} ion substitution and low-temperature sintering, the sample with x = 0.10 had excellent microwave dielectric properties ($\varepsilon_r = 6.28$, $Q \times f = 50400$ GHz, and $\tau_f = -145$ ppm/°C) for LTCC applications.

4. Conclusions

Zn^{2+}-substituted $Li_2(Mg_{1-x}Zn_x)SiO_4$ ceramics were synthesized by a traditional solid-state method. The use of a LiF sintering aid enabled the successful reduction in the sintering temperature of ceramics to 900 °C. Zn^{2+} ion doping could enhance dielectric properties of $Li_2(Mg_{1-x}Zn_x)SiO_4$ ceramics, including keep a low dielectric constant ($\varepsilon_r = 6.28$), high quality factor ($Q \times f = 50400$ GHz) and good temperature coefficient ($\tau_f = -145$ ppm/°C). This ceramic could be an alternative LTCC material for multilayer substrate for antenna and filter application. Furthermore, an increase in Zn^{2+} ion content resulted in a gradual increase in the temperature coefficient (τ_f) with a negative value range. The maximum value of τ_f was −120 ppm/°C, which could be improved by adding positive temperature coefficient material in the further researches.

Declaration of competing interest

The authors declare that they have no known competing financial interests or personal relationships that could have appeared to influence the work reported in this paper.

Acknowledgments

This work was supported by National Natural Science Foundation of China No. 52003256 and by Major Science and Technology projects in Sichuan Province No. 2019ZDZX0026 and by the Key projects of Sichuan Province No. 2020YFG0106, and by Foundation for University Teacher of Education of China No. ZYGX2019J011.

References

[1] Z.M. Temesvari, D. Maros, P. Kadar, Review of mobile communication and the 5G in manufacturing, Procedia Manuf. 32 (2019) 600–612.

[2] Y.M. Zhang, H.N. Li, S.Z. Huang, S. Fan, L.N. Sun, B.B. Tian, F.M. Chen, Y. Wang, Y. M. Shi, H.Y. Yang, Rechargeable aqueous zinc-ion batteries in $MgSO_4/ZnSO_4$ hybrid electrolytes, Nano-Micro Lett. 12 (1) (2020).

[3] Y. Yang, J. Li, H.W. Zhang, G. Wang, G.W. Gan, Y.H. Rao, Effects of Bi_2O_3-$MnO_{(2)}$ additives on tunable microstructure and magnetic properties of low temperature co-fired NiCuZn ferrite ceramics, J. Mater. Sci. Mater. Electron. 31 (15) (2020) 12325–12332.

[4] J. Li, Y. Yang, G. Wang, L. Guo, Y.H. Rao, G.W. Gan, H.W. Zhang, Enhanced structure and microwave magnetic properties of MgZn ferrite by Cd^{2+} ion substitution for LTCC applications, Ceram. Int. 46 (5) (2020) 6600–6604.

[5] Y. Yang, H.W. Zhang, J. Li, F. Xu, G.W. Gan, D.D. Wen, Effects of Bi_2O_3-Nb_2O_5 additives on microstructure and magnetic properties of low-temperature-fired NiCuZn ferrite ceramics, Ceram. Int. 44 (9) (2018) 10545–10550.

[6] A. Rose, B. Masin, H. Sreemoolanadhan, K. Ashok, T. Vijayakumar, Synthesis and microwave dielectric studies of pure Li_2MgSiO_4 and B_2O_3, MgF_2, WO_3 added Li_2MgSiO_4 for substrate applications, Appl. Surf. Sci. 449 (2018) 96–104.

[7] Z.H. Zhou, H. Su, X.L. Tang, H.W. Zhang, F. Xu, S. Zhang, Y.L. Jing, Microwave dielectric properties of LBBS glass added $(Zn_{0.95}Co_{0.05})_{(2)}SiO_4$ for LTCC technology, Ceram. Int. 42 (9) (2016) 11161–11164.

[8] V. Singh, S. Mahamuda, A.S. Rao, N. Singh, J.L. Rao, M. Irfan, Ultraviolet (UV)-B radiation from Gd3+ activated Li2MgSiO4 ceramics, Optik 207 (2020).

[9] R. Peng, H. Su, D. An, Y.C. Lu, Z.H. Tao, D.R.N. Chen, L. Shi, Y.X. Li, The sintering and dielectric properties modification of Li_2MgSiO_4 ceramic with Ni^{2+}-ion doping based on calculation and experiment, J. Mater. Res. Technol. 9 (2) (2020) 1344–1356.

[10] R. Peng, Y.X. Li, H. Su, Y.C. Lu, Y.R. Yun, Q. Zhang, S.J. Zhang, Effect of cobalt-doping on the dielectric properties and densification temperature of Li_2MgSiO_4 ceramic: calculation and experiment, J. Alloys Compd. 827 (2020).

[11] A. Rose, B. Masin, H. Sreemoolanadhan, K. Ashok, T. Vijayakumar, Effects of TiO_2 addition on microwave dielectric properties of Li_2MgSiO_4 ceramics, Mater. Res. Express 5 (3) (2018).

[12] S. Chen, X. Zhou, W.J. Song, J.B. Sun, H. Zhang, J.N. Jiang, L.H. Deng, S.J. Dong, X.Q. Cao, Mg_2SiO_4 as a novel thermal barrier coating material for gas turbine applications, J. Eur. Ceram. Soc. 39 (7) (2019) 2397–2408.

[13] A. Rose, B. Masin, K. Ashok, H. Sreemoolanadhan, T. Vijayakumar, Analysis on the influence of ZnO addition on microwave dielectric properties of Li_2MgSiO_4 ceramics, Bull. Mater. Sci. 42 (6) (2019).

[14] Z.J. Ye, J. Li, G. Wang, Z.F. Qi, G.W. Gan, Y. Yang, H.W. Zhang, Synthesis, phase composition and modified microwave dielectric properties of Mg^{2+} substituted Zn_2SiO_4 ceramics with uniform microstructure, Mater. Res. Express 6 (10) (2019).

[15] B.M. Moshtaghioun, D. Gomez-Garcia, J.I. Pena, Mg_2SiO_4-$MgAl_2O_4$ directionally solidified eutectics: hardness dependence modelled through an array of screw dislocations, J. Eur. Ceram. Soc. 40 (12) (2020) 4171–4176.

[16] A. Bigham, A.H. Aghajanian, S. Allandaneh, S.A. Hassanzadeh-Tabrizi, Multifunctional mesoporous magnetic Mg_2SiO_4-$CuFe_2O_4$ core-shell nanocomposite for simultaneous bone cancer therapy and regeneration, Ceram. Int. 45 (15) (2019) 19481–19488.

[17] Z.Z. Weng, C.X. Song, Z.X. Xiong, H. Xue, W.F. Sun, Y. Zhang, B. Yang, M.J. Reece, H.X. Yan, Microstructure and broadband dielectric properties of Zn_2SiO_4 ceramics with nano-sized TiO_2 addition, Ceram. Int. 45 (10) (2019) 13251–13256.

[18] C. Zhang, R.Z. Zuo, J. Zhang, Y. Wang, Structure-dependent microwave dielectric properties and middle temperature sintering of forsterite $(Mg_{1-x}Ni_x)_{(2)}SiO_4$ ceramics, J. Am. Ceram. Soc. 98 (3) (2015) 702–710.

[19] V.V. Dozmarov, L.D. Iskhakova, Y.A. Velikodnyi, L.G. Makarevich, A.V. Gaister, E. M. Dianov, Crystal growth and polymorphism of Li_2MgSiO_4, Crystallogr. Rep. 45 (6) (2000) 1059–1061.

[20] X.L. Jing, X.L. Tang, W.H. Tang, Y.L. Jing, Y.X. Li, H. Su, Effects of Zn^{2+} substitution on the sintering behaviour and dielectric properties of $Li_2Mg_{1-x}Zn_xSiO_4$ ceramics, Appl. Phys. A Mater. 125 (6) (2019).

[21] G. Dou, M. Guo, Y.X. Li, Effects of $CaTiO_3$ on microwave dielectric properties of Li_2ZnSiO_4 ceramics for LTCC, J. Mater. Sci. Mater. Electron. 27 (1) (2016) 359–364.